Peroxisome extensions deliver the *Arabidopsis* SDP1 lipase to oil bodies

Nelcy Thazar-Poulot[a], Martine Miquel[b], Isabelle Fobis-Loisy[a,1], and Thierry Gaude[a,1]

[a]Laboratoire de Reproduction et Développement des Plantes, Unité Mixte de Recherche 5667 Centre National de la Recherche Scientifique, Institut National de la Recherche Agronomique, Ecole Normale Supérieure de Lyon, Université Claude Bernard Lyon 1, 69364 Lyon Cedex 07, France; and [b]Institut Jean-Pierre Bourgin, Unité Mixte de Recherche 1318 Institut National de la Recherche Agronomique–AgroParisTech, Équipe de Recherche Labellisée CNRS 3559, Institut National de la Recherche Agronomique Centre de Versailles-Grignon, 78026 Versailles Cedex, France

Lipid droplets/oil bodies (OBs) are lipid-storage organelles that play a crucial role as an energy resource in a variety of eukaryotic cells. Lipid stores are mobilized in the case of food deprivation or high energy demands—for example, during certain developmental processes in animals and plants. OB degradation is achieved by lipases that hydrolyze triacylglycerols (TAGs) into free fatty acids and glycerol. In the model plant *Arabidopsis thaliana*, Sugar-Dependent 1 (SDP1) was identified as the major TAG lipase involved in lipid reserve mobilization during seedling establishment. Although the enzymatic activity of SDP1 is associated with the membrane of OBs, its targeting to the OB surface remains uncharacterized. Here we demonstrate that the core retromer, a complex involved in protein trafficking, participates in OB biogenesis, lipid store degradation, and SDP1 localization to OBs. We also report an as-yet-undescribed mechanism for lipase transport in eukaryotic cells, with SDP1 being first localized to the peroxisome membrane at early stages of seedling growth and then possibly moving to the OB surface through peroxisome tubulations. Finally, we show that the timely transfer of SDP1 to the OB membrane requires a functional core retromer. In addition to revealing previously unidentified functions of the retromer complex in plant cells, our work provides unanticipated evidence for the role of peroxisome dynamics in interorganelle communication and protein transport.

oil bodies | retromer | SDP1 lipase | peroxisome | protein trafficking

In seed plants, an essential function of seed reserves is to provide energy to the embryo for postgerminative growth until the seedling can perform photosynthesis. These reserves usually consist of storage proteins, carbohydrates, and lipids, with oil being the most common storage compound (1). The major storage lipids are triacylglycerols (TAGs), which are accumulated in subcellular structures called oil bodies (OBs). In *Arabidopsis thaliana*, OBs occupy 60% of the cell volume in the cotyledons of mature embryos and are located at the periphery of the cell (2). Upon seed germination, TAGs are hydrolyzed to release free fatty acids (FAs) and glycerol. Although the biochemical pathways that use glycerol and FAs to synthesize sugars are well documented, the initial step of oil degradation by TAG lipases has just started to be elucidated (3, 4). Although lipases have been purified from seeds of different plant species (5–7), physiological evidence for a function in TAG mobilization was clearly established only recently for the *A. thaliana* Sugar-Dependent 1 (SDP1) and SDP1-LIKE (SDP1L) lipases (8, 9). The *sdp1* mutant was isolated from a forward genetic screen based on the observation that mutants impaired in TAG mobilization failed to develop in the absence of an exogenous carbon source (8). Analysis of *sdp1* and *sdp1l* single and *sdp1 sdp1l* double mutants revealed that SDP1 activity accounts for the major degradation of TAGs after seed germination (9). SDP1 and SDP1L belong to the unorthodox class of patatin-like lipases similar to the mammalian and yeast lipases required for TAG breakdown (10). Although SDP1 was found to localize to the surface of OBs (8), it is unclear how SDP1 is targeted to OBs. Interestingly, *A. thaliana* mutants impaired in retromer functions

exhibit severe defects in seed and plant development, including alteration in the maturation of seed storage proteins and the presence of small OBs (11, 12). The retromer is a multiprotein complex, conserved among eukaryotes, that is involved in the recycling of transmembrane receptors and retrograde transport of cargo proteins from endosomes to the *trans*-Golgi network (13). In mammals, the retromer consists of two distinct subcomplexes: one composed of a dimer of Sorting Nexins (SNXs) and the other, known as the core retromer, consisting of a trimer of vacuolar protein sorting (VPS) 26, VPS29, and VPS35 proteins (13, 14). The *Arabidopsis* genome contains genes encoding all components of the retromer complex, including three *SNX* genes—designated *SNX1, SNX2a*, and *SNX2b*—three genes coding for VPS35 isoforms (*VPS35a, VPS35b*, and *VPS35c*), two genes encoding VPS26 isoforms (*VPS26a* and *VPS26b*), and a single gene encoding VPS29 (12, 15–17). Here, we show that core retromer mutants display defects in OB biogenesis and storage oil breakdown during postgerminative growth in *A. thaliana*. We also report that the TAG lipase SDP1 initially surrounds peroxisomes and then migrates to the surface of OBs through peroxisome tubulations. In the absence of a functional core retromer complex, SDP1 migration is delayed, suggesting a function for the retromer in mediating the timely transport of SDP1—and possibly other lipases—to the OB surface, which is an essential step for seed oil mobilization. In addition, our work provides unanticipated evidence for the role of peroxisome dynamics in interorganelle communication and protein transport.

Significance

Storage of lipids in oil bodies (OBs) and their subsequent degradation in response to developmental or environmental cues is a common behavior of eukaryotic cells. In *Arabidopsis* seeds, the major lipase implicated in OB degradation is Sugar-Dependent 1 (SDP1). We report that lipid storage and degradation are severely impaired in seeds of *Arabidopsis* mutants altered in the retromer function, a multiprotein complex involved in protein trafficking. We show that SDP1 is initially localized on peroxisomes and then migrates to the OB surface during the course of seedling growth. SDP1 translocation occurs through peroxisomal extensions, and a functional retromer allows timely transfer of SDP1 to OBs. Our work provides unanticipated evidence for the role of peroxisome dynamics in interorganelle communication and protein transport.

Results

Core Retromer Mutants Are Sugar-Dependent for Seedling Establishment. To investigate whether the small size of OBs in retromer mutants might be related to defects in seed oil storage or mobilization, we compared growth of wild-type (WT), *sdp1*, and retromer mutant seedlings in the presence or absence of sugar in the medium. The *snx* triple mutant, which lacks a functional SNX subcomplex, and WT seedlings showed ∼60 and 40% reduction of their primary root growth on a medium without sucrose, respectively (Fig. 1 *A–C* and Table S1). The *vps29* mutant exhibited a more severe post-germinative growth defect similar to that of *sdp1.4* and *1.5* mutants, with nearly 90% root length reduction. The *vps35a vps35c* double mutant also showed a diminution of root growth in the absence of sugar, although less severe than *vps29*. This latter finding may reflect the presence of a still partially functional core retromer implicating the remaining VPS35b isoform.

To ascertain that the vps phenotype was dependent on sugar availability, as is the case with *sdp1*, we attempted to rescue the postgerminative growth defect of the *vps29*, *sdp1.4*, and *sdp1.5* mutants by transferring mutant seedlings grown on a medium devoid of sugar for 8 d to a fresh medium containing 1% sucrose. Whereas 12-d-old mutants left in a medium without sugar displayed arrest of growth (Fig. S1*A*), resumption of growth was noticed for the three mutant seedlings after 4 d of growth in the sugar-supplemented

medium (Fig. S1*B*). These results indicate that the core retromer mutants are sugar-dependent for seedling establishment.

Core Retromer Mutants Are Affected in Lipid Storage and Mobilization. To determine whether the core retromer mutants are impaired in lipid reserve mobilization, we first examined OB morphology and degradation in the *vps29* mutant compared with *sdp1* and WT seedlings at different times after germination. Confocal microscopy observation of OBs stained with Nile Red revealed that from 4 to 7 d after germination (DAG) on medium without sucrose, the amount of OBs decreased in WT hypocotyls (Fig. 2 *A* and *G*) to become undetectable at 14 DAG (Fig. 2*J*). Contrary to WT seedlings, *vps29* and *sdp1* hypocotyls still displayed numerous OBs at 7 DAG (Fig. 2 *H* and *I*), with the size of *vps29* OBs being considerably smaller than those of WT (Fig. 2 *G* and *H*), whereas *sdp1* OBs were much larger (Fig. 2*I*). Although degradation of OBs did occur in mutants as deduced from the reduced number of OBs at 7 and 14 DAG (Fig. 2 *H*, *I*, *K*, and *L*), some OBs still remained undegraded in *vps29* and *sdp1* mutants at 14 DAG (Fig. 2 *K* and *L*). The persistence of OBs during late stages of seedling growth in the two mutants indicates that *vps29*, like *sdp1*, has a defect in lipid reserve breakdown.

We further analyzed the composition in FAs of germinating seeds. We found no major differences in long chain and very long chain FA (VLCFA) composition for WT and mutants (Fig. S2), with a percentage of VLCFAs related to total FAs (TFAs) of 27% in WT, 28% in *sdp1*, and 25% in *vps29* dry seeds, respectively. By contrast, the amount of total eicosenoic acid—a valuable marker to assess TAG content and hence OB breakdown in *A. thaliana* (18–20)—was significantly different between WT and mutant seeds, with >2 and 1.5 times more eicosenonic acid (C20:1) in WT than *vps29* and *sdp1* seeds, respectively (Fig. 2*M*). During the first 4 d of growth, ∼50% of C20:1 were degraded in WT seedlings, whereas only 32% and 37% were degraded in *vps29* and *sdp1* mutants, respectively. Interestingly, the two mutants showed similar patterns of degradation. Whereas degradation in the WT started slowly from 0 to 3 DAG and then increased sharply from 3 to 4 DAG, where 37% of eicosenoic acid was mobilized, degradation in *vps29* and *sdp1* was slow and approximately linear from 0 to 4 DAG. Together, these data suggest that lipid storage accumulation, as well as mobilization, are impaired in *vps29* in a way similar to *sdp1*.

Defects in lipid reserve mobilization can result from alteration of the hydrolysis of TAGs, such as in *sdp1*, or of the beta-oxidation process that occurs in peroxisomes (3). To determine which process is altered in *vps29*, we assessed whether the mutant was capable of converting indole-3-butyric acid (IBA) to indole-3-acetic acid, which is a peroxisomal mechanism analogous to FA beta-oxidation (21). To this end, we tested the sensitivity of mutant seedlings to IBA. In the presence of 30 μM IBA, both *vps29* and *sdp1* seedlings exhibited a strong reduction (>50%) of primary root elongation like WT seedlings (Fig. S3). These results imply that beta-oxidation is functional in *vps29* and suggest that the core retromer mutant, like *sdp1*, exhibits defects in TAG hydrolysis.

The SDP1 Lipase Migrates from Peroxisomes to the OB Surface Through Peroxisomal Tubulation. Because of phenotypic similarities between *vps29* and *sdp1* mutants, we wondered whether SDP1 might be mislocalized in the absence of a functional retromer complex. To explore the localization of SDP1 at the subcellular level, we transformed *A. thaliana* Col-0 and *vps29* mutant lines with a construct consisting of the *SDP1* genomic sequence fused to green fluorescent protein (GFP) under the control of the putative 5′ promoter region of *SDP1*. Unfortunately, the construct did not yield enough fluorescence to analyze SDP1–GFP localization. To circumvent this problem, we designed another construct allowing expression of a GFP–SDP1 fusion protein under the control of the constitutive 35S promoter. This construct was functional because, when introduced in the *sdp1* mutant, it rescued the sugar-dependent

Fig. 1. Sugar-dependent phenotype of retromer and *sdp1* mutants. (*A* and *B*) WT, retromer (*snx* triple, *vps29*, *vps35a vps35c*), *sdp1.4*, and *sdp1.5* mutant seedlings grown on MS medium with (*A*) or without (*B*) 1% (wt/vol) sucrose for 8 DAG. (Scale bar: 5 mm.) (*C*) Percentage of primary root length reduction induced by sugar deprivation. Values are mean ± SEM. Three independent experiments were performed, and a total of at least 42 seedlings were analyzed.
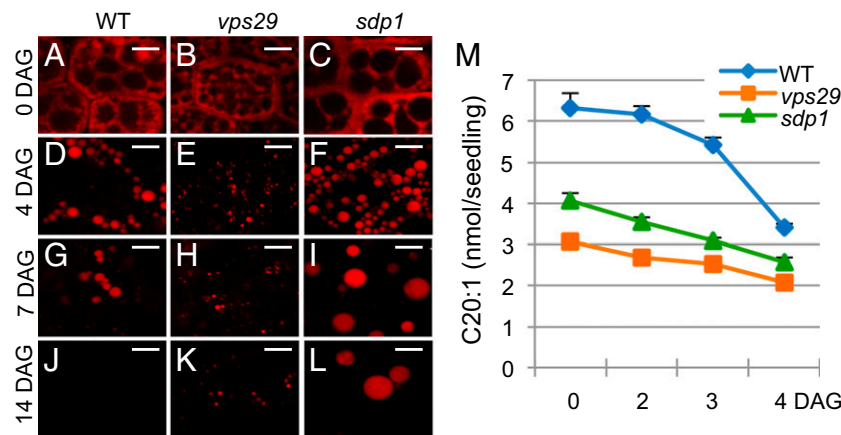
Fig. 2. OB morphology and TFA contents in WT, *vps29*, and *sdp1* mutants. (*A–L*) Detection of OBs in WT and mutant (*vps29, sdp1*) seeds and hypocotyl seedlings during postgerminative growth on MS medium without sucrose. Nile Red staining of OBs and confocal microscopy observation are shown for WT (*A, D, G,* and *J*), *vps29* (*B, E, H,* and *K*), and *sdp1* (*C, F, I,* and *L*). At least three independent experiments were performed for each kinetic point, and >10 seeds or seedlings were analyzed per experiment. (Scale bars: 5 μm.) (*M*) Quantification of C20:1 in dry seeds (0 DAG) and seedlings (2, 3, and 4 DAG) grown on MS medium with sucrose for WT, *vps29*, and *sdp1.4* mutants. Level of C20:1 is expressed in nmol per seed or seedling. Experiments were repeated twice on four to six samples of 20 dry seeds or 20 seedlings per germination time. Values are mean ± SEM.

phenotype (Fig. S4). In hypocotyls of 4-DAG WT seedlings, we found that GFP–SDP1 surrounded contiguous round-shaped compartments that were distinct from the Nile Red-stained OBs (Fig. 3*A*). The GFP–SDP1 labeling appeared heterogeneous in intensity, with the presence of highly fluorescent dots alternating with less intense fluorescent regions, resembling a string-like structure. Connections between the GFP–SDP1-labeled compartments, as well as with OBs, occurred through direct contact or via tubular structures. At 5 DAG, a major change happened with the relocalization of GFP–SDP1 toward the surface of OBs for 81% of WT hypocotyls analyzed (Fig. 3*C* and Fig. S5). Most OBs were adjacent to each other or, when distant, were linked by GFP–SDP1-labeled tubules. The relocalization of GFP–SDP1 toward the surface of OBs was observed in *vps29*, but was drastically delayed, with only 12% of hypocotyls exhibiting SDP1-surrounded OBs at 5 DAG and 72% of hypocotyls at 8 DAG. (Fig. 3 *B* and *D* and Fig. S5). The marked difference of GFP–SDP1 localization between the WT and *vps29* mutant lines suggests a role for VPS29 in the proper routing of SDP1 to OBs during seedling growth.

Because physical interactions between OBs and peroxisomes have been reported (22–25), we investigated whether the round-shaped compartments labeled with GFP–SDP1 might correspond to peroxisomes. To this end, we transformed the GFP–SDP1 line with mCherry–PTS1, a marker for peroxisomes (26). In 4-d-old hypocotyls of WT seedlings, a stage in which OBs are not surrounded by SDP1, we found that GFP–SDP1 associated with compartments labeled with mCherry–PTS1 (Fig. 3*E*) that were distinct from OBs because they were not stained with Nile Red. At this stage, GFP–SDP1 was also localized on the surface of peroxisomes in *vps29* hypocotyls (Fig. 3*F*). Thorough observation of seedlings coexpressing the GFP-labeled lipase and peroxisome marker allowed us to detect tubules displaying both fluorescent proteins, which indicates that these tubular structures are peroxisome extensions (Fig. 3*G*). Together, our data suggest that, during postgerminative growth, the lipase SDP1 is first associated with the surface of peroxisomes and then migrates to the surface of OBs, either through direct contact between peroxisomes and OBs or via tubular extensions of peroxisomes.

To monitor the translocation of SDP1 from peroxisomes to the OB surface, we used time-lapse imaging. In hypocotyls of 3-DAG WT seedlings, GFP–SDP1-labeled peroxisomes were close to OBs and quite immobile (Movie S1). By contrast, at 4 DAG, the GFP–SDP1-labeled peroxisomes became very mobile, with

the appearance of thin, long (7.4 ± 0.4 μm long; *n* = 149; Fig. S6) tubular extensions emerging from peroxisomes (arrowheads, Fig. 4 *A* and *B*), occasionally with several tubules extending from the same peroxisome (Fig. 4*B*). The tubular extensions could connect peroxisomes to each other and peroxisomes to OBs (Fig. 4). Peroxisomal tubules allowed translocation of GFP–SDP1 to the surface of OBs, eventually leading to the enwrapping of OBs with GFP–SDP1 (Fig. 4 *A* and *B* and Movie S2). In *vps29* hypocotyls, at the same developmental stage, GFP–SDP1 peroxisomes, although actively moving through the cytoplasm, produced fewer and shorter (2.7 ± 0.2 μm long; *n* = 51) tubular extensions that preferentially linked peroxisomes, but rarely came into contact with OBs (Fig. S6 and Movie S3). Nonetheless, we noticed that the translocation of GFP–SDP1 through peroxisomal tubules did occur in *vps29*, but with a delay of ~3 d (Fig. 3*D* and Movie S4). Together, these data indicate that the transport of SDP1 from peroxisomes toward the surface of OBs is mediated by tubular extensions whose fine-tuning requires a functional core retromer complex.

Discussion

Our analysis of null mutants for components of the retromer complex shows that the core retromer plays an active role in lipid storage, as well as in lipid mobilization, during postgerminative growth. Intriguingly, although both *sdp1* and *vps29* mutants share similar defects in lipid mobilization, FA composition, and sugar dependency for seedling growth, the size of their OBs greatly differs. We may suppose that proteins other that SDP1, and that participate in OB formation/organization, are possibly misrouted, underrepresented, or overrepresented at the surface of OBs in the retromer mutant, and that this might account for this size difference. The monitoring of eicosenoic acid levels during postgerminative growth unambiguously confirms the defect in lipid mobilization of *vps29* seedlings, a defect even stronger than that of *sdp1*. Remarkably, both *vps29* and *sdp1* dry seeds have reduced eicosenoic acid contents compared with WT seeds, indicating that the biosynthesis of storage lipids is also altered in these mutants. Considering the role of the core retromer in protein sorting and recycling, we may presume that proteins involved in the biosynthetic pathway of TAGs may be misrouted or have their lifetime affected in core retromer mutants. Although both *vps29* and *sdp1* seedlings are impaired in TAG degradation, they nonetheless retain the ability to hydrolyze a small amount of storage lipids, notably at early stages of development. We
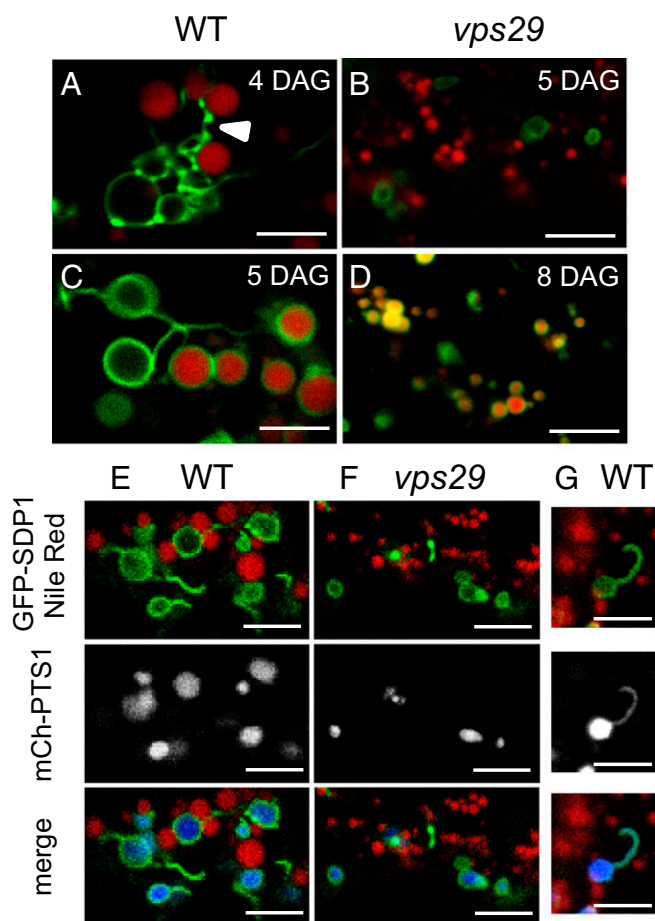
Fig. 3. SDP1 subcellular localization during postgerminative growth. (*A–D*) WT and *vps29* seedlings stably expressing GFP-SDP1 under the 35S promoter were grown on MS medium with 1% (wt/vol) sucrose. At 4, 5, or 8 DAG, seedlings were incubated in Nile Red and imaged by confocal microscopy to visualize OBs and SDP1 in hypocotyl cells. At 4 DAG, GFP–SDP1-labeled compartments (in green) are distinct from OBs (in red) in WT (*A*) and *vps29* (*B*) hypocotyls. At 5 DAG for WT (*C*) and 8 DAG for *vps29* (*D*), GFP–SDP1 labeling is found around the OBs. White arrowhead shows the string-like structure. For each time point, three independent experiments were performed, and at least five seedlings were analyzed per experiment. (*E–G*) Identification of SDP1-labeled compartments at young developmental stages. At 4 DAG, WT (*E* and *G*) or *vps29* (*F*) seedlings grown on MS medium with 1% (wt/vol) sucrose were incubated in Nile Red, and colocalization of GFP–SDP1 (in green), mCherry–PTS1 (peroxisome marker in gray or blue), and Nile Red (in red) was detected by confocal microscopy. Confocal sections in *G* show that SDP1-labeled tubular extensions colocalized with the peroxisome marker. At least 10 WT and *vps29* seedlings were analyzed. (Scale bars: 5 μm.)

noticed that this low rate of TAG hydrolysis, which is SDP1-independent, correlates with SDP1 association with peroxisomes, a location where the enzyme is likely not active. This low lipid mobilization nevertheless provides enough energy to allow the little postgerminative growth of mutant seedlings. Importantly, the timing of SDP1 relocation to OBs correlates with an increase in TAG hydrolysis, which suggests that SDP1 relocalization to OBs initiates its activity. We propose that, at early stages of postgerminative growth, SDP1 first localizes to the surface of peroxisomes, where it is inactive, and then moves to the surface of OBs, which triggers a burst in TAG hydrolysis to support seedling establishment. Surprisingly, we found that SDP1 relocalizes to OBs through peroxisomal tubules. Similar peroxisomal extensions have already been reported to occur in plant cells in response to hydroxyl stress, but their exact functions remain

unclear (27). Although close proximity of peroxisomes to OBs has already been described in various organisms (22, 23, 28), including the observation of peroxisomal extensions enwrapping OBs in yeast (25), to our knowledge a change in localization of lipases or any other proteins from peroxisomes to another intracellular compartment has never been reported. In mammalian cells, the two main lipases, Hormone Sensitive Lipase and Adipose Triglyceride Lipase (ATGL), are cytosolic proteins before being recruited at the surface of lipid droplets (29, 30). ATGL, although lacking a transmembrane domain, is predominantly found bound to membranes, and its delivery to lipid droplets involves a membrane trafficking pathway dependent on coatomer proteins (31). It is unclear why the plant SDP1 always seems to be associated with the surface of organelles. This finding might reflect some specific features of the SDP1 sequence regarding membrane association, either with particular lipids or structural proteins of these organelles. The temporal absence of SDP1–peroxisomal tubules in the *vps29* mutant, corresponding to the temporal inhibition of SDP1 transfer, indicates that the core retromer is a key element in mediating the formation of tubular structures required for the transport of SDP1 from peroxisomes to OBs. We may presume that peroxisome localization of SDP1 is a way to negatively regulate the lipase activity, so as to maintain OB integrity before the high needs of energy required at later stages of postgerminative growth. Thus, seed peroxisomes would act as a sequestration organelle for SDP1, transiently retaining the lipase away from its substrates and releasing it at later time points. This partitioning between enzyme and substrate illustrates the fine-tuning that exists between organelles to coordinate their respective activities.

Our results underscore the complexity of OB biogenesis and mobilization of lipid stores in seeds and reveal an unexpected dynamic of lipases during postgerminative growth. We also provide evidence for the role of peroxisomes in interorganelle communication and protein transport. Lastly, our work reveals the importance of the retromer trafficking machinery, both during OB formation, including accumulation of TAGs, and their degradation. How the retromer complex mediates peroxisome/OB communication and whether it may play similar roles, at least partially, in other model systems (e.g., yeast, human cells) remain particularly attractive to elucidate. Similarly, it would be particularly interesting to unravel whether peroxisomal tubulations are a common way to transport proteins between organelles in eukaryotic cells.

Experimental Procedures

Plant Materials and Growth Conditions. WT *A. thaliana* (Columbia accession) was obtained from the Nottingham *Arabidopsis* Stock Centre (University of Nottingham, Nottingham, United Kingdom). The *vps29.4* (Columbia accession no. GABI125H09) T-DNA mutant line has been described (15). *vps35 a-1 vps35c-1* (*vps35 a-1* SALK_039689, *vps35c-1* SALK_099735) was obtained from I. Hara-Nishimura (University of Kyoto, Kyoto). The *snx1-2 snx2a-2 snx2b-1* triple mutant (*snx1-2* SALK_03351, *snx2a-2* SALK_127971, *snx2b-1* GABI_105E07) has been described (12). *sdp1.4* (Columbia accession no. SALK_102887) and *sdp1.5* (Columbia accession no. SALK_076697) were obtained from P. Eastmond (University of York, York, United Kingdom). The mCherry–PTS1 construct was obtained from B. K. Nelson (University of Tennesse, Knoxville, TN). Seedlings were grown vertically on agar plates containing MS salts plus or minus 1% (wt/vol) sucrose in short-day light conditions (8 h of light and 16 h of dark).

Root Length Measurements and Beta-Oxidation Process. Primary root length was measured by using ImageJ software (NIH). Percentage of primary root length reduction was calculated as the average size of roots developed on sucrose containing medium minus the average size of roots grown in the absence of sucrose divided by the average size of roots developed on sucrose containing medium × 100. Thus, 100% of root length reduction would correspond to seedlings showing no primary root (0 mm) on medium deprived of sucrose.

For the beta-oxidation experiment, primary root elongation was quantified on seedlings grown for 7 d on MS medium with 1% (wt/vol) sucrose containing 30 μM IBA (Sigma).
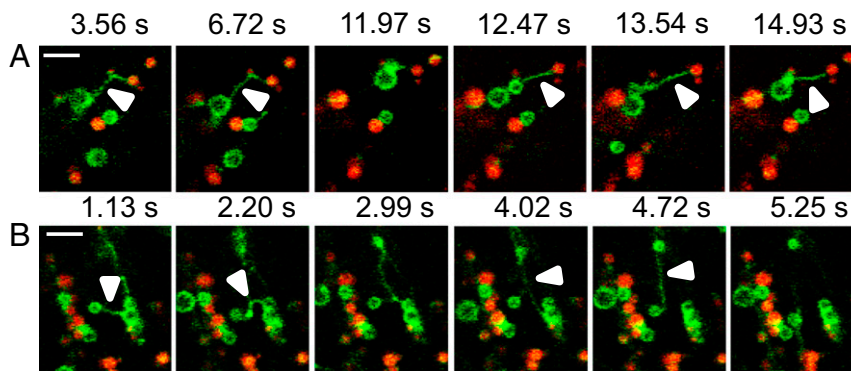
Fig. 4. Peroxisomal extensions allow transfer of SDP1 from peroxisomes to OBs. (*A* and *B*) WT GFP–SDP1 expressing seedlings at 4 DAG were treated with Nile Red and imaged by a spinning disk confocal microscope during 15 min. At this stage, SDP1 is only present on peroxisomes. (Scale bars: 5 µm.) (*A*) Arrowheads mark the tubular extensions protruding from peroxisomes (SDP1 labeling in green) and reaching OBs (red labeling). (*B*) Arrowheads mark tubules connecting two peroxisomes (SDP1 labeling in green). Images were extracted from Movie S2.

FA Content and Composition. TFAs from dry seeds and seedlings were directly transmethylated as described (1), except for some points. Heptadecanoic acid (C17:0) was used as an internal standard. FA methyl esters (ME) were extracted in hexane and separated by gas chromatography. Level of C20:1 was determined with the following calculation: [(area of C20:1 − ME/MW of C20:1 − ME) × (quantity of C17:0)/area of C17:0)]/seedling number. Experiments were repeated twice on four to six batches of 20 dry seeds or 20 seedlings per germination time.

SDP1 Cloning. The *SDP1* genomic sequence, including 1,883 bp of the putative promoter region (pSDP1::gSDP1), was amplified by PCR using the primer pair AttB1-pgSDP1-F1 (CGGGCTCCAAGAACCATAATCCCCG) and AttB2pgSDP1-R1 (TAGCATCTATAACACTACCAGACACC) and transferred by gateway recombination (Invitrogen) in the pMDC107 (32) for a GFP fusion at the C terminus of SDP1 (pSDP1::gSDP1–GFP).

The coding sequence (CDS) of SDP1 (from ATG to Stop codon) was amplified by PCR using the primer pair AttB1–SDP1 (ATGGATATAAGTAATGAG) and AttB2–SDP1 (CTAAGCATCTATAACACTACC). PCR products were cloned in pDonZeo (Invitrogen). SDP1 CDS was transferred by gateway recombination (Invitrogen) in the pK7WGF2 vector (Functional Genomics Division of the Department of Plant Systems Biology, Ghent, Belgium) for fusion of GFP to the

N terminus of SDP1 (p35S::GFP-cdsSDP1). Transgenic plants for SDP1 tagged with GFP were generated as described (33).

Nile Red Staining and Confocal Microscopy. *Arabidopsis* seedlings grown on MS plates were stained with Nile Red (0.33 µg/mL; Molecular Probes) (34) and observed under a spectral-SP5 confocal microscope (Leica). For Nile Red/GFP colocalization experiments, samples were excited at 488 nm, Nile Red emission was recovered between 571 and 590 nm, and GFP emission was between 500 and 520 nm. For Nile Red/GFP/mCherry labeling, samples were sequentially excited at 488 and 561 nm, and emission was recovered between 503 and 515 nm (GFP), between 555 and 571 nm (Nile Red), and between 597 and 606 nm (mCherry). Movies were taken with a spinning disk confocal system (Leica). The frame rate is one image per 2 s.

1. Li Y, Beisson F, Pollard M, Ohlrogge J (2006) Oil content of Arabidopsis seeds: The influence of seed anatomy, light and plant-to-plant variation. *Phytochemistry* 67(9):904–915.
2. Baud S, Dubreucq B, Miquel M, Rochat C, Lepiniec L (2008) Storage reserve accumulation in Arabidopsis: Metabolic and developmental control of seed filling. *Arabidopsis Book* 6:e0113.
3. Graham IA (2008) Seed storage oil mobilization. *Annu Rev Plant Biol* 59:115–142.
4. Quettier AL, Eastmond PJ (2009) Storage oil hydrolysis during early seedling growth. *Plant Physiol Biochem* 47(6):485–490.
5. Maeshima M, Beevers H (1985) Purification and properties of glyoxysomal lipase from castor bean. *Plant Physiol* 79(2):489–493.
6. Lin YH, Huang AH (1984) Purification and initial characterization of lipase from the scutella of corn seedlings. *Plant Physiol* 76(3):719–722.
7. Ncube I, Gitlesen T, Adlercreutz P, Read JS, Mattiasson B (1995) Fatty acid selectivity of a lipase purified from Vernonia galamensis seed. *Biochim Biophys Acta* 1257(2):149–156.
8. Eastmond PJ (2006) SUGAR-DEPENDENT1 encodes a patatin domain triacylglycerol lipase that initiates storage oil breakdown in germinating Arabidopsis seeds. *Plant Cell* 18(3):665–675.
9. Kelly AA, Quettier AL, Shaw E, Eastmond PJ (2011) Seed storage oil mobilization is important but not essential for germination or seedling establishment in Arabidopsis. *Plant Physiol* 157(2):866–875.
10. Athenstaedt K, Daum G (2006) The life cycle of neutral lipids: Synthesis, storage and degradation. *Cell Mol Life Sci* 63(12):1355–1369.
11. Shimada T, et al. (2006) AtVPS29, a putative component of a retromer complex, is required for the efficient sorting of seed storage proteins. *Plant Cell Physiol* 47(9):1187–1194.
12. Pourcher M, et al. (2010) Analyses of sorting nexins reveal distinct retromer-subcomplex functions in development and protein sorting in Arabidopsis thaliana. *Plant Cell* 22(12):3980–3991.
13. Attar N, Cullen PJ (2010) The retromer complex. *Adv Enzyme Regul* 50(1):216–236.
14. Wassmer T, et al. (2009) The retromer coat complex coordinates endosomal sorting and dynein-mediated transport, with carrier recognition by the trans-Golgi network. *Dev Cell* 17(1):110–122.
15. Jaillais Y, et al. (2007) The retromer protein VPS29 links cell polarity and organ initiation in plants. *Cell* 130(6):1057–1070.
16. Vanoosthuyse V, Tichtinsky G, Dumas C, Gaude T, Cock JM (2003) Interaction of calmodulin, a sorting nexin and kinase-associated protein phosphatase with the Brassica oleracea S locus receptor kinase. *Plant Physiol* 133(2):919–929.
17. Oliviusson P, et al. (2006) Plant retromer, localized to the prevacuolar compartment and microvesicles in Arabidopsis, may interact with vacuolar sorting receptors. *Plant Cell* 18(5):1239–1252.
18. Fulda M, Schnurr J, Abbadi A, Heinz E, Browse J (2004) Peroxisomal Acyl-CoA synthetase activity is essential for seedling development in Arabidopsis thaliana. *Plant Cell* 16(2):394–405.
19. Lemieux B, Miquel M, Somerville C, Browse J (1990) Mutants of Arabidopsis with alterations in seed lipid fatty acid composition. *Theor Appl Genet* 80(2):234–240.
20. Eastmond PJ, et al. (2000) Postgerminative growth and lipid catabolism in oilseeds lacking the glyoxylate cycle. *Proc Natl Acad Sci USA* 97(10):5669–5674.
21. Zolman BK, Yoder A, Bartel B (2000) Genetic analysis of indole-3-butyric acid responses in Arabidopsis thaliana reveals four mutant classes. *Genetics* 156(3):1323–1337.
22. Hayashi Y, Hayashi M, Hayashi H, Hara-Nishimura I, Nishimura M (2001) Direct interaction between glyoxysomes and lipid bodies in cotyledons of the Arabidopsis thaliana ped1 mutant. *Protoplasma* 218(1-2):83–94.
23. Schrader M (2001) Tubulo-reticular clusters of peroxisomes in living COS-7 cells: Dynamic behavior and association with lipid droplets. *J Histochem Cytochem* 49(11):1421–1429.
24. Goodman JM (2008) The gregarious lipid droplet. *J Biol Chem* 283(42):28005–28009.
25. Binns D, et al. (2006) An intimate collaboration between peroxisomes and lipid bodies. *J Cell Biol* 173(5):719–731.
26. Nelson BK, Cai X, Nebenführ A (2007) A multicolored set of in vivo organelle markers for co-localization studies in Arabidopsis and other plants. *Plant J* 51(6):1126–1136.
27. Sinclair AM, Trobacher CP, Mathur N, Greenwood JS, Mathur J (2009) Peroxule extension over ER-defined paths constitutes a rapid subcellular response to hydroxyl stress. *Plant J* 59(2):231–242.
28. Walther TC, Farese RV, Jr (2009) The life of lipid droplets. *Biochim Biophys Acta* 1791(6):459–466.

29. Granneman JG, et al. (2007) Analysis of lipolytic protein trafficking and interactions in adipocytes. *J Biol Chem* 282(8):5726–5735.
30. Miyoshi H, et al. (2006) Perilipin promotes hormone-sensitive lipase-mediated adipocyte lipolysis via phosphorylation-dependent and -independent mechanisms. *J Biol Chem* 281(23):15837–15844.
31. Soni KG, et al. (2009) Coatomer-dependent protein delivery to lipid droplets. *J Cell Sci* 122(Pt 11):1834–1841.

32. Curtis MD, Grossniklaus U (2003) A gateway cloning vector set for high-throughput functional analysis of genes in planta. *Plant Physiol* 133(2):462–469.
33. Jaillais Y, Fobis-Loisy I, Miège C, Rollin C, Gaude T (2006) AtSNX1 defines an endosome for auxin-carrier trafficking in Arabidopsis. *Nature* 443(7107): 106–109.
34. Greenspan P, Mayer EP, Fowler SD (1985) Nile red: A selective fluorescent stain for intracellular lipid droplets. *J Cell Biol* 100(3):965–973.

PLANT BIOLOGY